

## Catalytic Degradation of 4-Nitrophenol Using Gamma Irradiated PVA/Ag Nanocomposites.

Wael H. Eisa<sup>a,\*</sup>, Farag A. Ali<sup>b</sup>, Mohamed S. Sadek<sup>c</sup>

<sup>a</sup>Spectroscopy Department, Physics Division, National Research Center (NRC), Egypt)

<sup>b,c</sup>Menoufia University, Faculty of Science, Chemistry Department, Egypt)

### Abstract

In this work, PVA/Ag nanocomposites were prepared by adding different volumes of AgNO<sub>3</sub> to PVA solution. PVA/Ag nanocomposites used as a catalyst for the degradation of 4-nitrophenol (4-NP) to 4-aminophenol (4-AP). The responsive catalyst is easily synthesized, environmentally compatible, cost-effective and can be easily recovered by handling from the aqueous solution. The shape and particle size distribution were studied using Transmission Electron Microscope (TEM). The X-Ray diffraction (XRD) and UV-visible Absorption Spectra of Gamma-irradiated PVA/AgNO<sub>3</sub> Films were studied.

**Keywords:** PVA/Ag nanocomposites; 4-nitrophenol; TEM; XRD; UV-Visible.

### I. Introduction

Nitroaromatic compounds are used in many industrial processes, including the preparation of pesticides, explosives, textiles and paper. Therefore, these compounds are often detected as water pollutants as a result of their release in industrial effluents [1]. Remediation of wastewaters containing these pollutants is very difficult, since they are usually resistant to biological degradation [2]. Among these nitroaromatic compounds, nitrophenols are common pollutants. Nitrophenols (NPs) are the most common organic pollutants in industrial and agricultural effluents. *P*-Nitrophenol has been widely used in the production of pesticides, herbicides, dyes, and other industrial chemicals. On the other hand, 4-nitrophenol is an important intermediate for the manufacture of analgesic and antipyretic drugs [3]. As a result of these widespread applications, wastewaters and water resources, including groundwater and surface waters, have become contaminated with this compound.

Many processes have been developed for phenolic compounds removal such as adsorption, microbial degradation, photocatalytic degradation, electrocoagulation and electrochemical treatment and so on [4].

In recent years, nanophase materials have gained more attention because of special physical and chemical features. Zerovalent metals such as silver nanoparticles with the features of large volume to area ratio are a well-known catalytic material. [5]. Reductive degradation of pollutants using zerovalent Ag NPs which, is used as a heterogeneous catalyst, inspire researchers due to many benefits such as high rate of reaction and efficiency, non-toxicity,

insolubility, mild reaction conditions, and requirement for minimal follow-up treatment.

However, the use of Ag NPs in the degradation of pollutants is hindered with several obstacles. The most common challenges in dealing with these nanomaterials are mass transport, difficulties in separation and recycling as well as possible environmental and health risks caused by the potential release of nanoparticles into the environment [6].

Though catalytic processes may be performed in homogeneous systems, in the case of expensive catalysts such as those involving highly efficient precious and strategic metals like silver, it is important to recover the metals at the end of the process. For this reason, supported catalysis involving immobilization of the catalyst onto suitable support materials has been extensively investigated in the last few decades. Various types of support materials such as carbon, alumina and silica have been used for the immobilization of zerovalent metals [7]. Owing to their high cost and selectivity problems, researchers have directed their attention towards development of polymeric materials including natural biopolymers as supports for catalyst preparation. This also prevents metal leaching due to stabilization of the metal on the catalyst caused by metal-polymer interactions [8].

Herein, we make use of the prepared PVA/Ag nanocomposites, for the first time, as a catalyst for the degradation of 4-nitrophenol (4-NP). Compared with other polymeric nanocomposites, the responsive catalyst is easily synthesized, environmentally compatible, cost-effective and can be easily recovered by handling from the aqueous solution.

Facile synthesis of responsive catalysts is a challenge and interest to both industrial and academic researchers.

## II. Materials and methods

### 2.1. Materials

Silver nitrate ( $\text{AgNO}_3$ ) was purchased from Merck Co. 4-nitrophenol ( $4\text{-C}_6\text{H}_5\text{NO}_3$ ) was purchased from LOBA CHEMIE, India. Polyvinyl alcohol with an average molecular weight of 14,000 g/mol was obtained from Laboratory Rasayan, India. It was in the form of powder, partially hydrolyzed and used without further purification. All reagents were of analytical grade and used without further purification. All solutions were prepared using deionized water.

### 2.2. Preparation of the PVA/Ag nanocomposites

The samples were prepared according the method described elsewhere [9]. In a typical preparation procedure, 3 g of PVA was first dissolved in 50 mL of deionized water at 85 °C with magnetic stirring for about 5 hr until clear solution is obtained. Different volumes of 0.1 M  $\text{AgNO}_3$  solution was added to 10 ml of PVA solution with continuous stirring for about 1 hr to insure well homogeneity of the solution. The pH of the solution was adjusted to 4 using 0.1 M  $\text{HNO}_3$  to avoid the spontaneous reduction. Finally, the solution was casted on a Petri dish, left to dry in darkness to form the desired film and then the film was stripped from the dish.

The as-prepared samples were subjected to gamma irradiation using a Gamma cell 220 Excel 60Co irradiation facility (manufactured by MDS Nordion, Canada).

### 2.3. Analysis techniques

The UV-vis spectra measurements were recorded using V-630 UV-Vis spectrophotometer (Jasco, Japan). The crystalline and phase structures were determined by using X-ray diffraction XRD-DI series, Shimadzu apparatus using nickel-filter and Cu-K target ( $\lambda=1.5406 \text{ \AA}$ ). The shape and particle size distribution were studied using JEOL JEM 2010 Transmission Electron Microscope operated at 100 kV accelerating voltage. The silver concentration measurement was carried out using atomic absorption spectrometer Varian SpectrAA (220) with graphite furnace accessory and equipped with deuterium arc background corrector.

### 2.4. Gel content% determination

1×1 cm of Polymeric nanocomposite films were cut into pieces and then accurately weighed, ( $W_1$ ). The samples were then immersed in deionized water

for 6 h at room temperature for sol extraction. The swollen samples were removed from the solvent and dried in an oven at 40-50 °C until a constant weight was reached ( $W_2$ ). The gel content% is calculated according to the following relation:

$$\text{Gel content\%} = (W_2/W_1) \times 100$$

### 2.5. Catalytic reduction of 4-nitrophenol

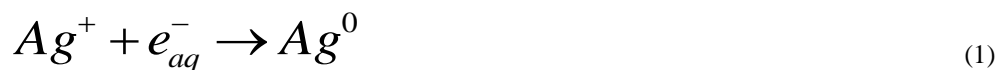
A typical experiment was carried out as follows; 2.77 ml of water was mixed with 25  $\mu\text{l}$  ( $10^{-2}$  M) of 4-NP solution and 200  $\mu\text{l}$  of freshly prepared  $\text{NaBH}_4$  solution ( $10^{-1}$  M). A square piece of nanocomposite film (0.9 cm side length) was taken into the bottom of quartz cuvette of path length 1 cm. The catalytic activity was followed by a UV-vis spectrophotometer with recording the decrease of the absorption peak at 403 nm in UV-vis spectra and a simultaneous increase in absorption at 300 nm, indicating the formation of 4-AP.

## III. Results and Discussion

### 3.1. The UV-visible Absorption Spectra of Gamma-irradiated PVA/ $\text{AgNO}_3$ Films.

The effect of  $\gamma$ -irradiation upon the prepared composites film of PVA loaded with different  $\text{Ag}^+$  concentrations manifested itself through an interesting color variation i.e. the investigated samples showed a distinct color variation ranged from colorless, faint yellow and yellowish brown depending on the loading level of  $\text{Ag}^+$  ions. Fig. 1 showed the UV-visible absorption spectra of 50 kGy  $\gamma$ -irradiated PVA films loaded with different concentrations of  $\text{AgNO}_3$ . The spectra showed absorption bands in the visible region related to the surface plasmon resonance [10]. The plasmon peak was intensified, narrowed and shifted to the lower energy side of the spectrum i.e. smaller particles are formed. These observations indicated that, under the same irradiation dose, excess  $\text{Ag}^+$  ions can assist the growth of Ag NPs and lead to increasing particle size.

The radiolytic reduction has been proven to be a powerful tool to produce monosized and highly dispersed metallic clusters [11]. The absorbed radiation energy in the media resulted in the formation of reactive species such as hydrated electron ( $e_{\text{aq}}$ ), hydrogen atom radical ( $\text{H}\cdot$ ) and hydroxyl radical ( $\text{OH}\cdot$ ). Among these species, ( $e_{\text{aq}}$ ) and ( $\text{H}\cdot$ ) are very powerful reducing agents, hence both of them reduce  $\text{Ag}^+$  ions within the PVA binder into metallic silver according to the reactions 1 and 2 [12]. This mechanism avoids the use of additional reducing agents and the following side reactions.



The PVA chain plays a significant role in avoiding the aggregation and/or agglomeration. Several active –OH groups in PVA are capable of adsorbing metal ions through secondary bonds and steric hindrance [13]. A reaction of metal ions ( $M^+$ ) with PVA that leads to their associations can be expressed as:



The load of excess  $AgNO_3$  into PVA matrix made the silver ions closer to each other which facilitated the growth of the Ag nanoparticles by consuming more  $Ag^+$  ions. This result was confirmed by the red shift of the absorption band.

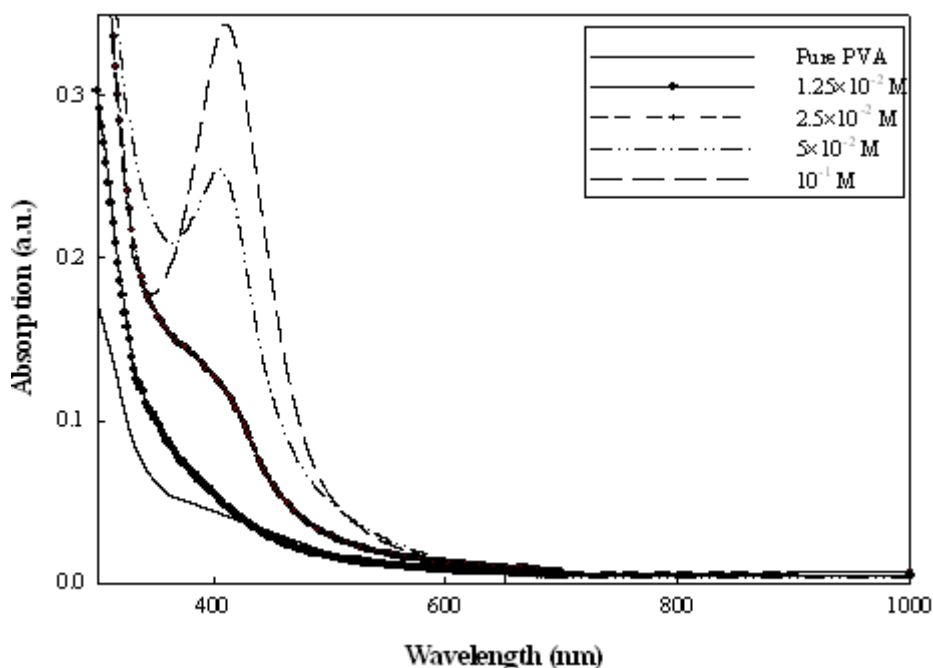


**Fig.1** UV–visible spectra of PVA/Ag nanocomposites loaded with different  $AgNO_3$  concentrations and irradiated with 50 kGy gamma radiation.

### 3.2. TEM of Ag Nanoparticles Grown from Different $AgNO_3$ Concentrations under 50 kGy Gamma Irradiation Dose.

The TEM of the prepared Ag NPs from different concentrations of  $AgNO_3$  under constant gamma irradiation dose (50 kGy) are presented in Fig. 2. A number of well-dispersed nanoparticles can clearly be seen in the TEM picture with external spherical shape and are to a large extent well-separated from one another. The average diameter of the nanoparticles is indicated as the peak position of the Gaussian curve of the histogram. Regarding to the histogram, the particle size is enlarged from 16.5 to 21.5 nm as the  $AgNO_3$  concentration increases from  $2.5 \times 10^{-2}$  to  $10^{-1}$  M. the particles exhibit a uniform shape and a very narrow size distribution as can be seen from the width of the Gaussian peak.

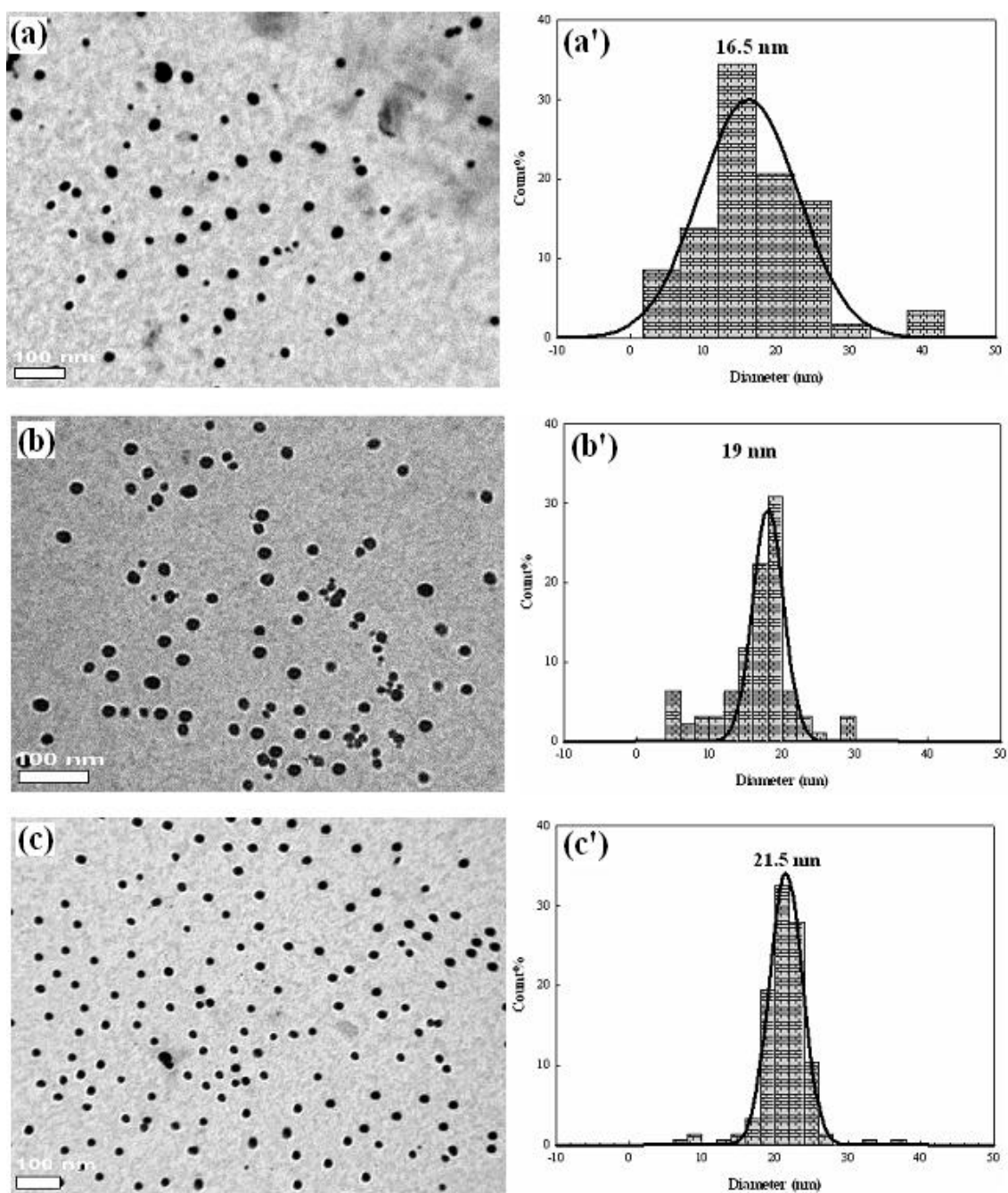


**Fig. 2** (a) TEM image of Ag nanoparticles grown from (a)  $2.5 \times 10^{-2}$ , (b)  $5 \times 10^{-2}$  and (c)  $10^{-1}$  M  $\text{AgNO}_3$  within PVA matrix under 50 kGy gamma irradiation doses and (a', b' and c') are the Gaussian fitting of the particle size distribution histogram.

### 3.3. X-ray Diffraction Patterns of $\gamma$ -irradiated PVA/Ag Nanocomposites loaded with different $\text{AgNO}_3$ content.

The peaks for  $2\theta$  values at 38, 44, 64.5 and 77.42° pertaining to Ag nanoparticles which indicates the reduction of the Ag salt in the polymer matrix (see Fig. 3). The discernible peaks can be indexed to the planes (111), (200), (220) and (311) respectively corresponds to face centre cubic structure of silver according to JCPDS (No.4-0783). The XRD peaks of cubic Ag were broad in accordance with their small grain size and low degree of crystallinity.

The particle size 'D' is calculated based on the regular broadening of XRD peaks as a function of decreasing crystallite size. This broadening is a fundamental property of XRD described by well-established Scherer theory [14].

$$D = k\lambda / \beta \cos \theta$$

where  $\beta$  full width at half maximum of the peak corresponding to plane (111),

k is the so-called shape factor which usually takes a value of about 0.9, and

$\theta$  is the angle obtained from  $2\theta$  value corresponding to maximum intensity peak in XRD pattern.

The  $\text{AgNO}_3$  concentration is determining factor in controlling the particle size. When an excess of  $\text{AgNO}_3$  is used in the synthesis, the average nanocrystal diameter is significantly increased from 11 to 18 nm.

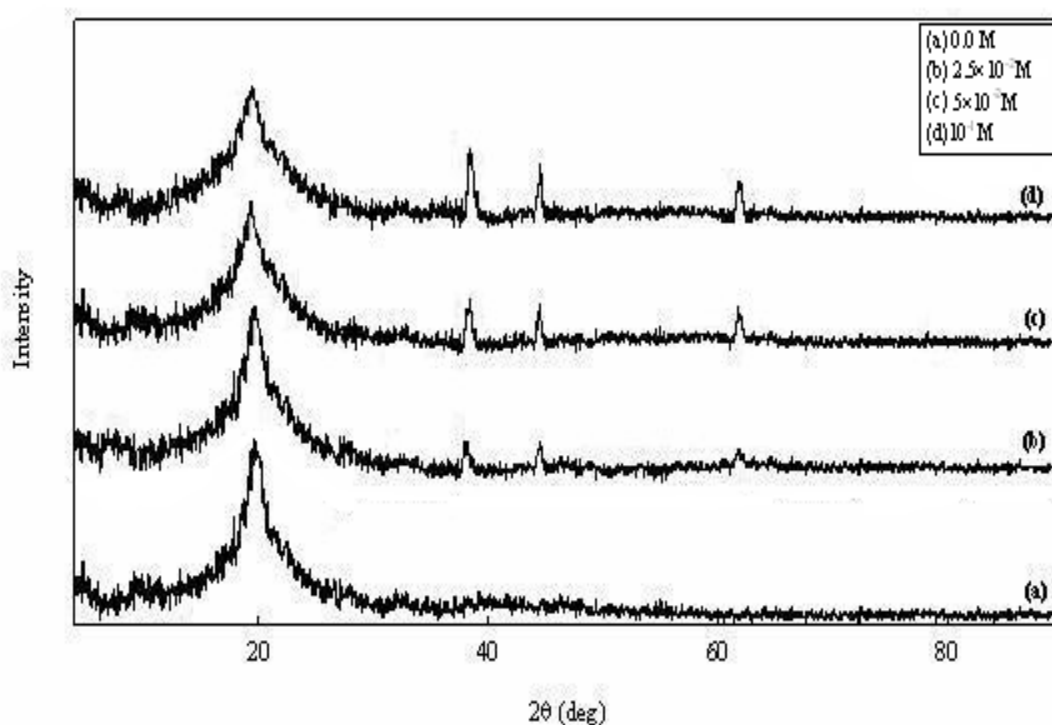


**Fig. 3** The X-ray diffraction patterns of unirradiated PVA films filled with different molar concentrations of  $\text{AgNO}_3$ .

### 3.4. Gel Content Percent and Crosslinking Density Determination

The effect of gamma radiation on gel fraction of PVA/Ag nanocomposites is shown in Fig. 4. It is apparent that the gel fraction of PVA/Ag nanocomposites increased with radiation dose. These results imply the existence of irradiation-induced crosslinking in PVA. This can be attributed to the formation of a three dimensional network structure upon irradiation [15]. Furthermore, another factor which has a great effect on gel content of PVA is the  $\text{AgNO}_3$  concentration in the polymer matrix. This idea could be monitored from the gel content against  $\text{AgNO}_3$  concentration as presented in Fig. 12. It can be seen that the gel content increased markedly with the increasing of  $\text{AgNO}_3$  content. This is may be due to the reduced Ag nanoparticles are crosslinked by radiation and we expect that Ag is not segregated from the polymer network structure during the swelling experiment.

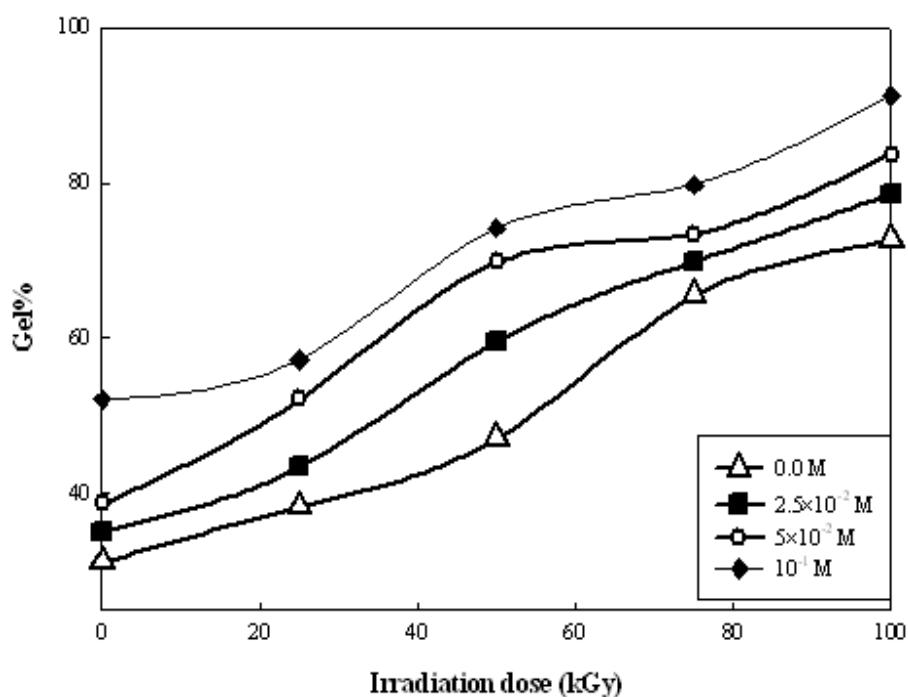
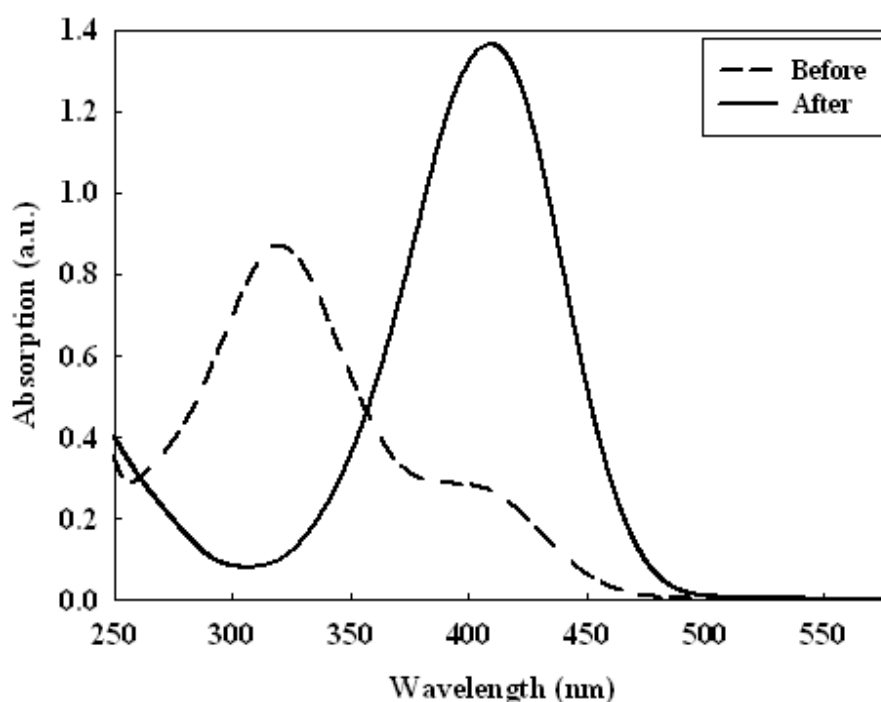


Fig. 4 gel content % against the irradiation dose of PVA containing different concentrations of  $\text{AgNO}_3$ .

### 3.5. Catalytic activity of PVA/Ag Nanocomposite Film.

The enhancement of the solvent resistance of the polymer as well as success of immobilization of the Ag NPs within the polymer matrix have inspired us to make use of the PVA/Ag nanocomposite films in catalytic reduction of 4-nitrophenol which is highly toxic material. In this experiment, the 100 kGy gamma irradiated PVA/Ag film prepared from 0.1 M  $\text{AgNO}_3$  was used.

The aqueous 4-nitrophenol solution showed two absorption peaks; an intense peak at 319 nm related to 4-NP and a broad peak at 403 nm corresponded to small amount of 4-nitrophenolate ions in the system (see Fig. 5) [16]. The UV-vis spectrum of 4-NP (Fig. 6) showed a significant change upon the addition of the  $\text{NaBH}_4$  as a reducing agent. It could be seen that the spectrum was dominated with a sharp absorption peak at 403 nm which is due to the formation of 4-nitrophenolate ion in the basic medium [17]. It is worth to mention that the absorption peak of the 4-nitrophenolate ions do not show considerable variation either in intensity and/or position without adding the Ag NP to the reaction medium (see Fig. 7). It was reported that, aromatic nitro compounds are inert to the reduction of  $\text{NaBH}_4$  in the absence of a catalyst [18,19].



**Fig. 5** UV-vis absorption spectra of 4-NP before and after addition of NaBH<sub>4</sub>.

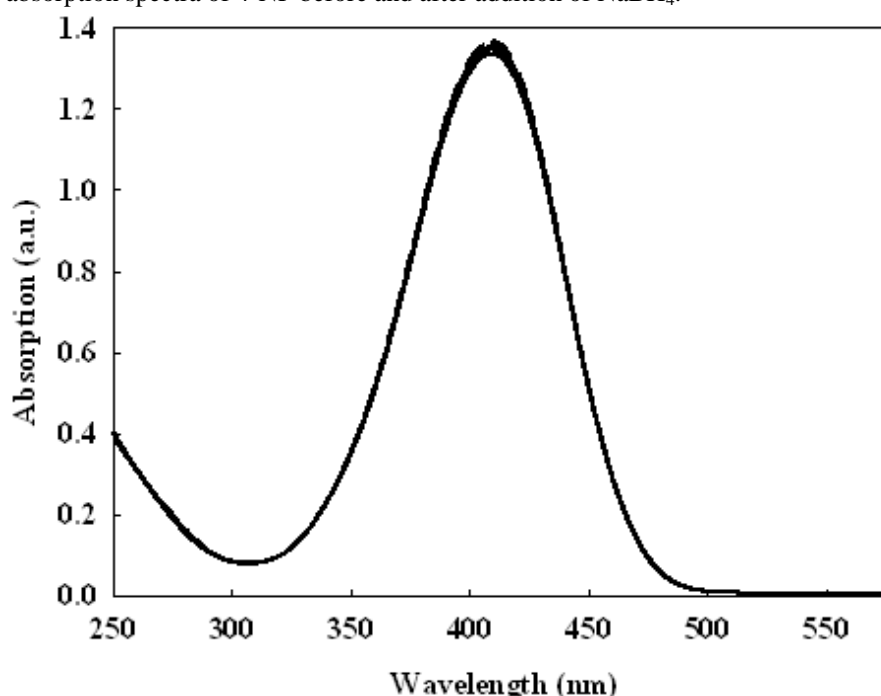


**Fig. 6** UV-Vis spectra of reaction systems recorded every 2 hours without catalyst (PVA/Ag nanocomposites)

In order to evaluate the catalytic activity of the prepared PVA/Ag nanocomposites on the reduction of 4-nitrophenol (4-NP) to 4-aminophenol (4-AP) by NaBH<sub>4</sub> as a model reaction, the reduction process was monitored by time-resolved UV-vis absorption spectra as shown in Fig. 7. After NaBH<sub>4</sub> was introduced into the 4-NP solution in the presence of PVA/Ag nanocomposites, the solution color diminished and the characteristic absorption peak of 4-nitrophenolate ion at 400 nm decreased gradually, while a new peak at 302 nm ascribed to the 4-AP was appeared.

Three runs were consecutively carried out to evaluate the efficacy of reusing the PVA/Ag catalyst as displayed in Fig. 7. It is observed that the time needed to complete the catalytic degradation reaction increases

from the first to the third run. The catalytic reaction completed within 18 min for the first run, while the third run shows much slower catalytic process (42 min).

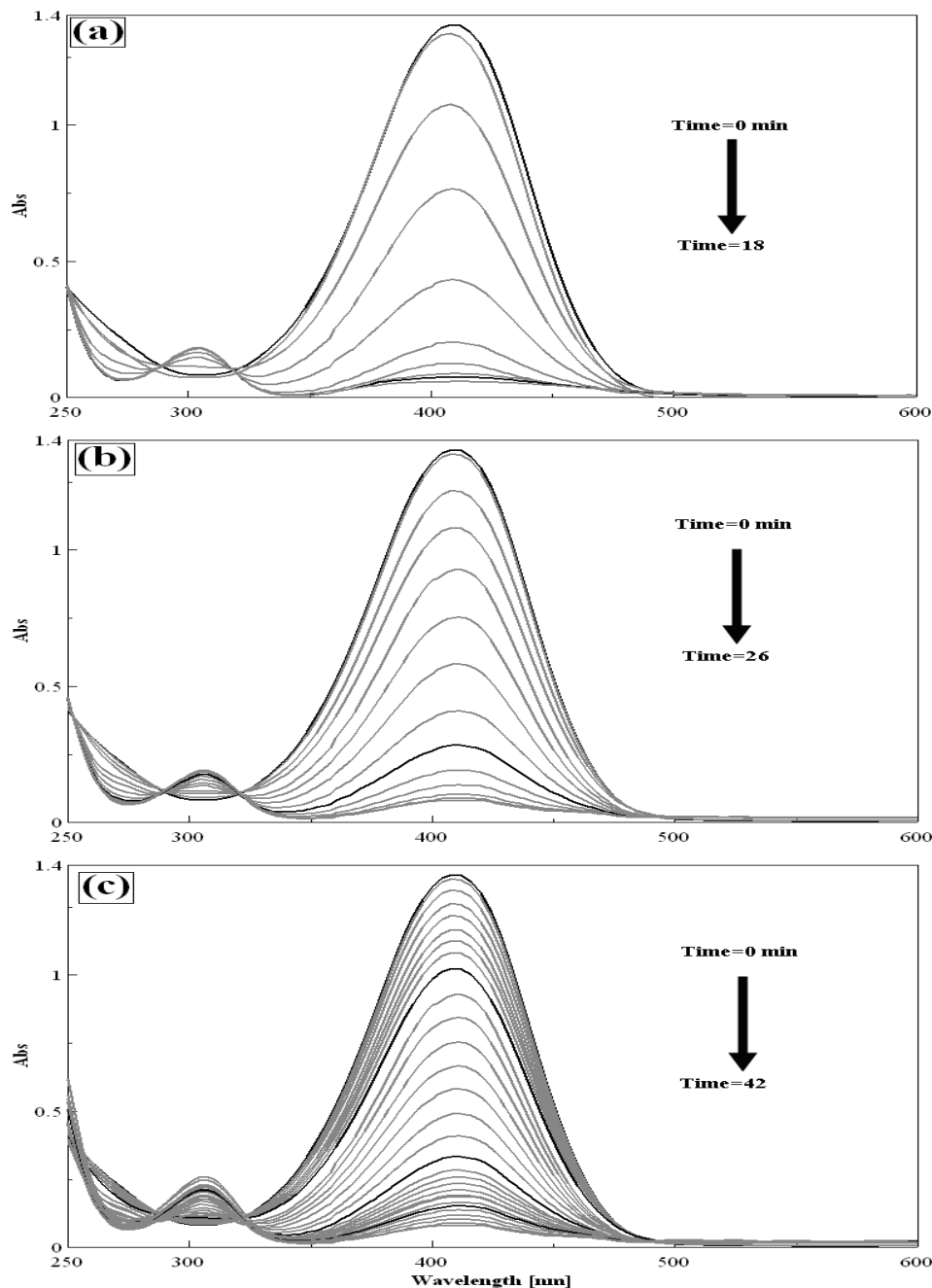


**Fig. 7** Time-dependent UV-vis absorption spectra for catalytic degradation of 4-NP by PVA/Ag nanocomposites for (a) first, (b) second and (c) third run.

Since the catalytic reduction reaction was carried in large excess concentration of  $\text{NaBH}_4$  as compared with that of 4-NP, the rate constant ( $K$ ) could be assumed to be independent of  $\text{NaBH}_4$  concentration. Hence, the catalytic reduction reaction is considered as pseudo-first-order kinetics with respect to 4-NP concentration. The rate constant ( $K$ ) of the catalytic reaction can be estimated by the following relation [47];

$$\frac{dC_t}{dt} = KC_t \text{ or } \ln\left(\frac{C_t}{C_0}\right) = \ln\left(\frac{A_t}{A_0}\right) = -Kt \quad (1)$$

where  $C_0$  and  $C_t$  are the concentration of 4-NP at the beginning and time  $t$  of the reaction while  $A_0$  and  $A_t$  are their corresponding absorptions, respectively.

Fig. 8 shows the graphical plots of  $\ln(A_t/A_0)$  vs the reaction time ( $t$ ). The plots presented a good linear relationship between  $\ln(A_t/A_0)$  and the reaction time ( $t$ ). The slopes of these relations determines the rate constant ( $K$ ) of the reaction. Figure 16 represented a good linear relation of  $\ln(A)$  versus time. The estimated reaction rate constant was estimated to be  $3.5 \times 10^{-3} \text{sec}^{-1}$  for the 1<sup>st</sup> run;  $2.2 \times 10^{-3} \text{sec}^{-1}$  for the 2<sup>nd</sup> run;  $9.7 \times 10^{-4} \text{sec}^{-1}$  for the 3<sup>rd</sup> run. As can be seen from Fig. 8, the reaction rate is found to be lowered after the first run, and is lowered even more during the 3<sup>rd</sup> run. This may be attributed to the passivation of the Ag nanoparticles and hence the less ability to catalyze the reaction.

The atomic absorption spectrometry was used to determine the traces of Ag NPs that segregated from the polymer network during the catalytic degradation experiment after each run. The obtained results showed that no Ag NPs were leached from the PVA matrix confirming the success of Ag NPs immobilization within PVA chains.

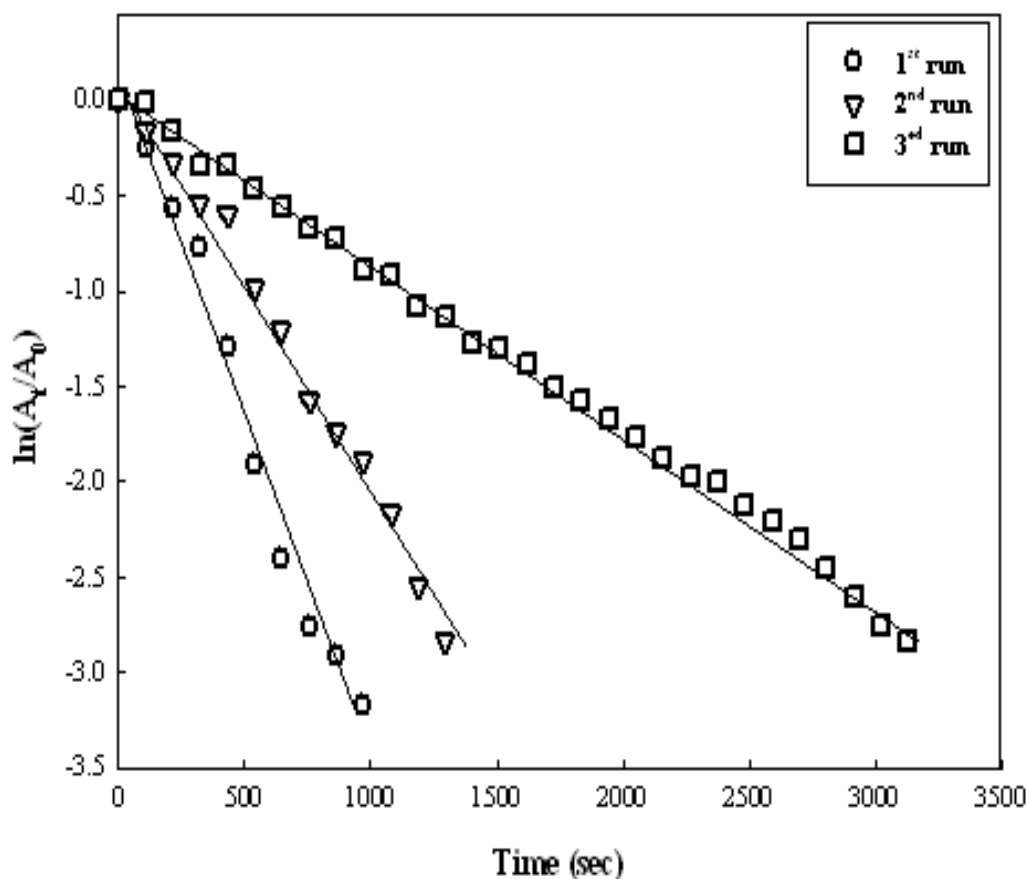


Fig. 8 A plot of  $\ln(A_t/A_0)$  versus time for the catalytic reduction of 4-NP to 4-AP by  $\text{NaBH}_4$  in the presence of PVA/Ag nanocomposite film.

#### IV. Conclusion

PVA/Ag nanocomposites are proved to be an efficient candidate for the reduction of nitroaromatic compounds. The effect of  $\gamma$ -irradiation upon the prepared composites film of PVA loaded with different  $\text{Ag}^+$  concentrations is cleared via the color variation i.e. from colorless to faint yellow and yellowish brown depending on the loading level of  $\text{Ag}^+$  ions. This indicates that under the same irradiation dose, excess  $\text{Ag}^+$  ions can help in growing of Ag NPs and increasing particle size.

#### References

- [1] P. Gharbani, M. Khosravi, S. M. Tabatabaiee, K. Zare, S. Dastmalchi, and A. Mehrizad, "Degradation of trace aqueous 4-chloro-2-nitrophenol occurring in pharmaceutical industrial wastewater by ozone, *International Journal of environmental science and technology*, 7(2), 2010, 377–384.
- [2] O. A. O'Connor and L. Y. Young, "Toxicity and anaerobic biodegradability

- of substituted phenols under methanogenic conditions,” *Environmental Toxicology and Chemistry*, 8(10), 1989, 853–862.
- [3] Y.-C. Chang and D.-H. Chen, “Catalytic reduction of 4-nitrophenol by magnetically recoverable Au nanocatalyst,” *Journal of Hazardous Materials*, 165(1–3), 2009, 664–669.
- [4] M. A. Lazar, S. Varghese, and S. S. Nair, “Photocatalytic water treatment by titanium dioxide: recent updates,” *Catalysts*, 2( 4), 2012, 572–601.
- [5] M. Venkatesham, D. Ayodhya, A. Madhusudhan, N. Veera Babu, and G. Veerabhadram, “A novel green one-step synthesis of silver nanoparticles using chitosan: catalytic activity and antimicrobial studies,” *Applied Nanoscience*, 4(1), 2014, 113–119.
- [6] L. Yuan, M. Yang, F. Qu, G. Shen, and R. Yu, “Seed-mediated growth of platinum nanoparticles on carbon nanotubes for the fabrication of electrochemical biosensors,” *Electrochimica Acta*, 53(10), 2008, 3559–3565.
- [7] J. P. Vyjayanthi, “Immobilization of nanoscale zerovalent metals for the reductive removal of recalcitrant pollutants,” *International Journal of Environmental Science and Technology*, 2( 4), 2012, 2173–2183.
- [8] L. M. Rossi, M. A. S. Garcia, L. L. R. Vono, Recent Advances in the Development of Magnetically Recoverable Metal Nanoparticle Catalysts,” *The Journal of the Brazilian Chemical Society*, 23, 2012, 1959-1971.
- [9] W. H. Eisa, Y. K. Abdel-Moneam, Y. Shaaban, A. A. Abdel-Fattah, and A. M. Abou Zeid, “Gamma-irradiation assisted seeded growth of Ag nanoparticles within PVA matrix,” *Materials Chemistry and Physics*, 128(1), 2011, 109–113.
- [10] M. F. Zayed, W. H. Eisa, and A. A. Shabaka, “ Malva parviflora extract assisted green synthesis of silver nanoparticles,” *Spectrochimica Acta Part A: Molecular and Biomolecular Spectroscopy*, 98, 2012 , 423–428.
- [11] J. L. Marignier, J. Belloni, M. O. Delcourt, and J. P. Chevalier, “Microaggregates of non-noble metals and bimetallic alloys prepared by radiation-induced reduction,” *Nature*, 8, 1985, 344–345.
- [12] S. P. Ramnani, J. Biswal, and S. Sabharwal, “Synthesis of silver nanoparticles supported on silica aerogel using gamma radiolysis,” *Radiation Physics and Chemistry*, 76(8), 2007, 1290–1294.
- [13] A. Gautam, P. Tripathy, and S. Ram, “Microstructure, topology and X-ray diffraction in Ag-metal reinforced polymer of polyvinyl alcohol of thin laminates,” *Journal of materials science*, 41( 10), 2006, 3007–3016.
- [14] R. Georgekutty, M. K. Seery, and S. C. Pillai, “A highly efficient Ag-ZnO photocatalyst: synthesis, properties, and mechanism,” *The Journal of Physical Chemistry C*, 112(35), 2008, 13563–13570.
- [15] B. Wongsuban, K. Muhammad, Z. Ghazali, K. Hashim, and M. Ali Hassan, “The effect of electron beam irradiation on preparation of sago starch/polyvinyl alcohol foams,” *Nuclear Instruments and Methods in Physics Research Section B: Beam Interactions with Materials and Atoms*, 211( 2), 2003, 244–250.
- [16] M. F. Zayed and W. H. Eisa, “Phoenix dactylifera L. leaf extract phytosynthesized gold nanoparticles; controlled synthesis and catalytic activity.,” *Spectrochimica acta. Part A, Molecular and biomolecular spectroscopy*, 121, 2014, 238–44.
- [17] A. Gangula, R. Podila, L. Karanam, C. Janardhana, and A. M. Rao, “Catalytic reduction of 4-nitrophenol using biogenic gold and silver nanoparticles derived from Breynia rhamnoides,” *Langmuir*, 27(24), 2011, 15268–15274.
- [18] D. M. Dotzauer, J. Dai, L. Sun, and M. L. Bruening, “Catalytic membranes prepared using layer-by-layer adsorption of polyelectrolyte/metal nanoparticle films in porous supports,” *Nano letters*, 6(10), 2006, 2268–2272.
- [19] N. Pradhan, A. Pal, T. Pal, Silver nanoparticle catalyzed reduction of aromatic nitro compounds,” *Colloids and Surfaces A: Physicochemical and Engineering Aspects*, 196, 2002, 247–257.